

Review

Porphyrins as light harvesters in the dye-sensitised TiO₂ solar cell

Wayne M. Campbell^a, Anthony K. Burrell^b, David L. Officer^{a,*}, Kenneth W. Jolley^a

^a *Nanomaterials Research Centre and The MacDiarmid Institute for Advanced Materials and Nanotechnology,
Massey University, Palmerston North, New Zealand*

^b *Actinide, Catalysis and Separations Chemistry, C-SIC, Los Alamos National Laboratory, Los Alamos, NM 87545, USA*

Received 5 December 2003; accepted 30 January 2004

Available online 10 June 2004

Contents

Abstract	1363
1. Introduction	1364
1.1. The dye-sensitised solar cell	1364
1.2. Porphyrins as light harvesting dyes in the DSSC	1366
2. Experimental	1370
2.1. Porphyrin syntheses	1370
2.2. The test cell	1370
2.3. Testing procedure	1370
2.3.1. TiO ₂ electrode preparation	1370
2.3.2. Dye adsorption	1370
2.3.3. Platinum counter electrode preparation	1370
2.3.4. Cell assembly and electrolyte introduction	1370
2.3.5. Calibration of light source and testing	1370
2.3.6. Data acquisition	1370
2.3.7. Results analysis and errors	1371
3. Results and discussion	1371
3.1. Initial test cell and chromophore optimisation	1371
3.2. Comparison of β - and <i>meso</i> -substituted monoporphyrim carboxylic acids	1372
3.3. Array porphyrins	1373
3.3.1. "Branched" and "linear" arrays	1373
3.3.2. "Sticky" porphyrin arrays	1374
3.4. <i>o,m,p</i> -Carboxylic acids	1374
3.5. Arylporphyrin substituents (TPP versus TXP versus TBP)	1374
3.6. Electrolyte influence	1375
3.7. Binding groups	1376
3.8. Linker conjugation	1377
3.9. Quantitative Grätzel cell results	1378
4. Conclusion	1378
Acknowledgements	1379
References	1379

Abstract

The sensitisation of TiO₂ with a wide variety of inorganic and organic dyes for light harvesting has been investigated over the last 20 years for the development of efficient solar cells. Given their efficacy in photosynthesis, porphyrin dyes have great potential in this regard. A significant number of porphyrins have been evaluated in photoelectrochemical cells (PECs), but little is known about the structural and electronic features

Abbreviations: AM1.5, air mass = 1.5 (1000 W m⁻²); BCMPP, biscalboxyphenyl-bismethoxyphenylporphyrin; BCPP, biscalboxyphenylporphyrin; DSSC, dye-sensitised solar cell; FF, fill factor; *I*_{sc}, short-circuit current; IPCE, incident monochromatic photon-to-current conversion efficiency; MP, *meso*-porphyrin; PEC, photoelectrochemical cell; SC, semiconductor; SS, steady state; TAP, tetraarylporphyrin; TBP, tetrakis(bis-3,5-*t*-butyl)porphyrins; TCP, tetrakis(4-carboxyphenyl)porphyrins; T3CPP, tetrakis(3-carboxyphenyl)porphyrins; T3,5CPP, tetrakis(bis-3,5-carboxy)porphyrins; TPP, tetraphenylporphyrin; TSPP, tetrasulphonylphenylporphyrin; TXP, tetraarylporphyrin; UP, uroporphyrin; *V*_{oc}, open circuit voltage; η , overall solar light energy conversion efficiency

* Corresponding author. Tel.: +64-6-3505918; fax: +64-6-3505612.

E-mail address: d.officer@massey.ac.nz (D.L. Officer).

required for efficient porphyrin light harvesting on semiconductors (SCs). One of the most appealing aspects of the use of porphyrins as dyes is that a wide variety of large porphyrin arrays can now be synthesised. The attachment of such arrays (or light harvesting antennae) to SCs such as TiO_2 provides the potential to dramatically increase the dye surface coverage of the SC, and therefore the dye-sensitised solar cell (DSSC) efficiency. There has been little work carried out in this area to date. Following the development of an efficient building block approach to functionalised porphyrin arrays, we have synthesised a variety of β -carboxylic substituted porphyrin monomers and multi-porphyrin arrays and evaluated their performance in the dye-sensitised TiO_2 (Grätzel) solar cell. The effect of porphyrin substituent, functional group position, linker conjugation, binding group and electrolyte on the porphyrin light harvesting efficiency was investigated. It was found that a β -substituted monoporphyrin carboxylic acid derivative with a conjugated linker shows significant advantage over any antennae-type of multi-porphyrin arrays. In particular, of all the porphyrins evaluated, 4-*trans*-2'-(2''-(5'',10'',15'',20''-tetraphenylporphyrinato zinc(II)yl)ethen-1'-yl)-1-benzoic acid gives an overall efficiency of 4.2% under AM1.5 conditions in an unoptimised Grätzel cell, making it one of the most efficient porphyrin dye sensitisers synthesised to date.

© 2004 Elsevier B.V. All rights reserved.

Keywords: Porphyrin; Solar cell; Titanium dioxide; TiO_2 ; PEC; DSSC

1. Introduction

1.1. The dye-sensitised solar cell

Nanoporous, nanocrystalline semiconductor (SC)-based dye-sensitised solar cells (DSSCs), although a relatively new technology [1], have demonstrated laboratory conversion efficiencies of up to 10.4% [2] and represent a promising method for the large scale conversion of renewable energy from the sun into electricity. The most successful DSSC is the commonly known Grätzel cell, using Ru-polypyridyl based dyes (Fig. 1) adsorbed on nanocrystalline films of titanium dioxide (TiO_2) [3].

Optimally, a dye for a DSSC should absorb across the entire visible spectrum, bind strongly to the semiconductor surface, have a suitably high redox potential for regeneration following excitation and be stable over many years of exposure to sunlight. The Ru-polypyridyl complexes utilised by Grätzel come close to fulfilling these requirements, although sensitisation at a number of wavelengths could certainly be improved. As for light harvesting in photosynthesis, in which a number of chlorophylls and carotenoids are involved in light collection, it is likely that optimal photosensitisation in DSSCs will only occur using a mixture of dyes. In addition, ruthenium complexes are likely to become increasingly more expensive as the demand for Ru raw materials increases. Consequentially, a wide variety of dyes

with differing binding groups and linkers (Fig. 2) have been tested as photosensitisers in the Grätzel cell.

Anchoring to TiO_2 has been achieved through a number of functional groups, such as salicylate, carboxylic acid, sulphonic acid, phosphonic acid and acetylacetonate derivatives, the most widely used and successful to date being the carboxylic acid and phosphonic acid functionalities.

The carboxylic acid groups, while ensuring efficient adsorption of the dye on the surface also promote electronic coupling between the donor levels of the excited chromophore and the acceptor levels of the TiO_2 SC. Some of the possible modes of chelation/derivatisation, ranging from chemical bonding (chelating or bridging mode) to H-bonding, are shown in Fig. 3. Falaras proposes that IR and Raman spectra support chemical bonding through ester formation **B** on the surface [14]. Duffy et al. [15], on the other hand, strongly suggest surface coordination involves *syn-syn* bridging between two surface titanium atoms **D**, whilst Ma et al. [16], with their studies on porphyrin dye systems using IR evidence, maintain that both **C** and **D** binding is involved. However, recently Weng et al. [17], using a new interface-sensitive molecular probe method with all-*trans*-retinoic acid, showed that 63% of surface binding arises from ester formation **B**, 34% from chelating **C** and bridging **D**, and 3% from anion **A** and hydrogen bonding **E**, **F**.

There is little information about the binding mode of phosphonic acid derivatives in the literature, although an ester type formation has been proposed [18,19] (Fig. 4). The photosensitiser $\text{Ru}(\text{PO}_3\text{-terpy})(\text{Me}_2\text{bpy})(\text{NCS})$, which shows a monochromatic and overall light-to-electrical conversion efficiency comparable to Ru dicarboxypolypyridyl-based complexes (Fig. 2A), binds strongly to the TiO_2 surface (about 80 times more strongly than carboxylated analogues), and, unlike the COOH anchoring group, is not displaced easily by water. The adsorbed state is maintained over a wide pH domain (pH = 0–9) with excellent solar cell performance.

The type of anchor functionality and linker between the sensitiser and SC surface can enhance electronic coupling and/or alter the surface state energetics so that electron in-

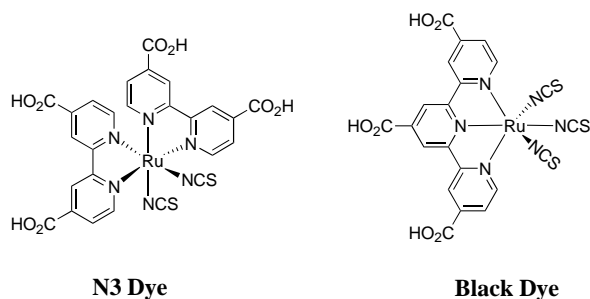


Fig. 1. Ru-polypyridine photosensitisers used by Grätzel.

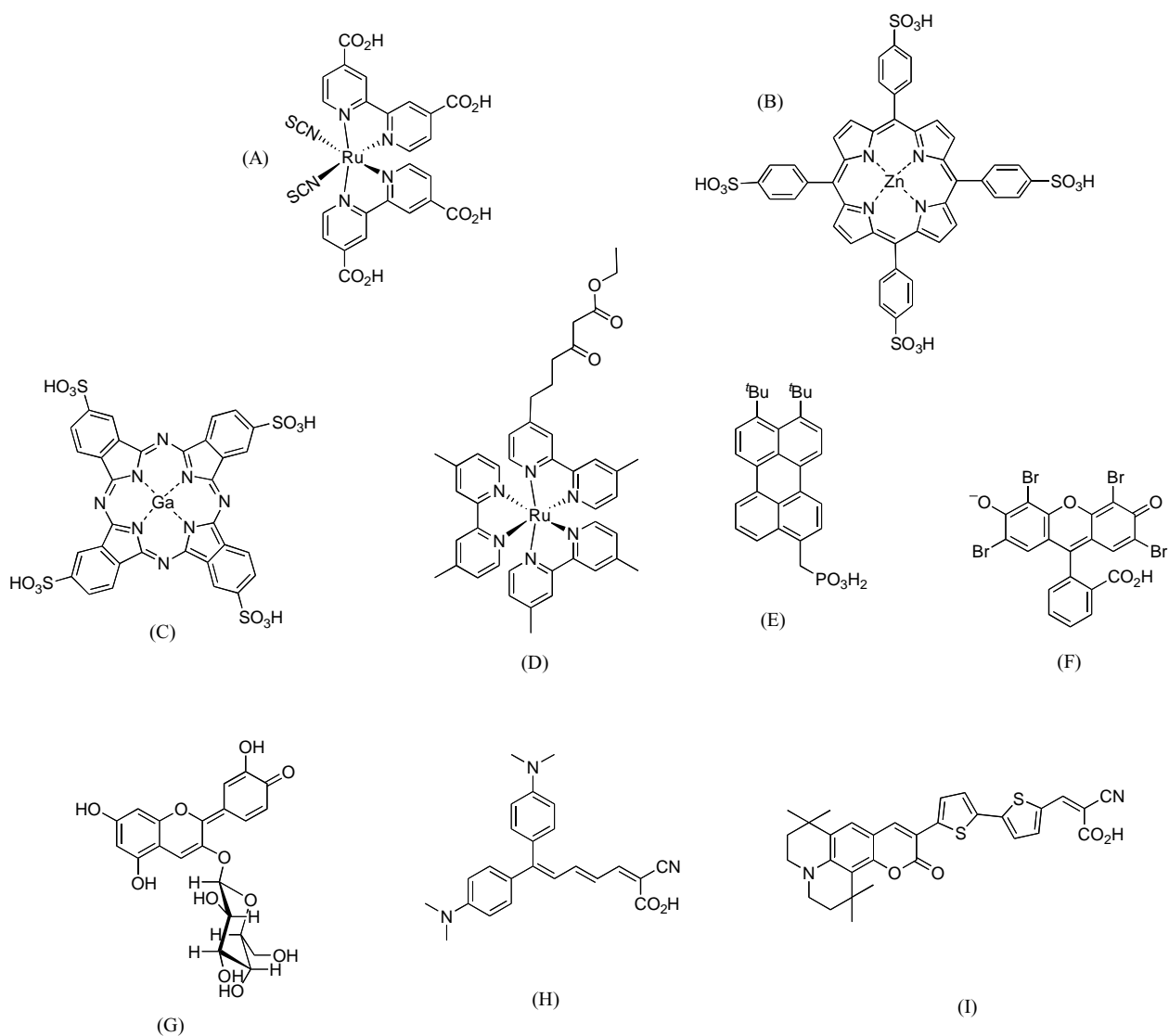


Fig. 2. Chromophores and anchoring systems used on TiO_2 . Ruthenium carboxypolypyridine complex **N3** (A) [4], zinc tetrasulphonatophenylporphyrin (B) and gallium tetrasulphonatophthalocyanine (C) [5], ruthenium acetylacetonate polypyridine complex (D) [6], perylene dye (E) [7], xanthene dye (Eosin Y) (F) [8–10], natural flavonoid anthocyanin dye extracted from California blackberries (G) [11], polyene dye NKX-2569 (H) [12], coumarin based NKX-2677 (I) [13].

jection is faster and more efficient. However, experiments suggest that the distance of the chromophoric ligand from the surface is critical to the design of molecular sensitizers, more so than the type of anchor [6]. For example, on TiO_2 , a Ru(II) polypyridyl sensitizer containing an *n*-propyl spacer between a bipyridine ring and an acetylacetonate group (Fig. 5A), gave comparable corrected incident monochro-

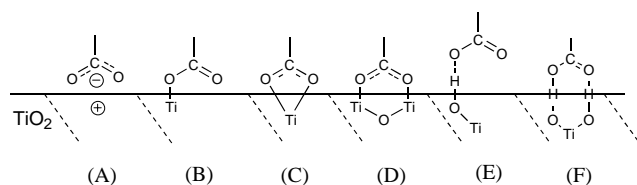


Fig. 3. Possible binding modes for carboxylic acid groups on TiO_2 .

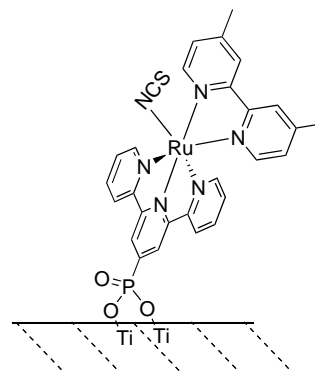


Fig. 4. Possible mode of phosphonic acid ester surface binding on TiO_2 [18,19].

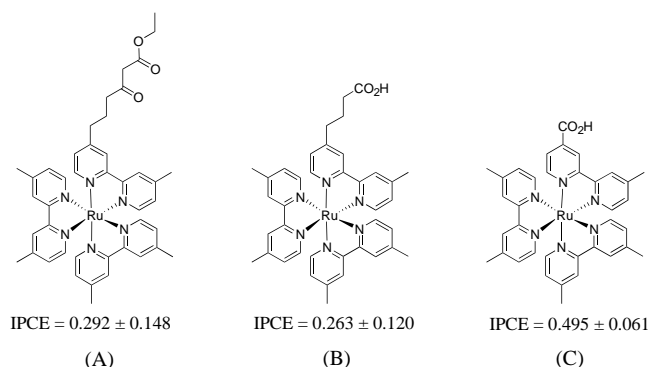


Fig. 5. IPCE_{max} values for model Ru-polypyridyl complexes [6].

matic photon-to-current conversion efficiency (IPCE) [20] values to one with a carboxylic acid group bound to the *n*-propyl spacer (Fig. 5B). Both of these dyes, however, have an IPCE_{max} value that is only about half of that when there is no *n*-propyl spacer present (Fig. 5C).

This result suggests that there may be an optimum sensitizer orientation (or distance from surface) and linker (e.g. length, conjugation) dependence, wherein interfacial charge separation is still efficient but the charge recombination is inhibited enough to give high IPCE values [6]. To date, the best organometallic dye is the Ru-based Black Dye (Fig. 1) of Grätzel that has an overall solar light energy conversion efficiency (η) [20] of 10.4% under AM1.5 conditions [2]. However, recently, a new very promising purely organic-based (coumarin bithiophene linked) dye (Fig. 2I) has been reported that gives an AM1.5 η value of 7.7% [13].

1.2. Porphyrins as light harvesting dyes in the DSSC

The use of porphyrins as light harvesters on SCs is particularly attractive given their primary role in photosynthesis and the relative ease with which a variety of covalent or noncovalent porphyrin arrays can be constructed. The attachment of a large porphyrin array to a nanocrystalline SC surface provides a way to dramatically increase the surface dye concentration and therefore, the light energy conversion efficiency of the device. Various porphyrins have been used for the photosensitization of wide-band-gap SCs like NiO, ZnO and TiO₂, the most common being the free-base and zinc derivatives of the *meso*-benzoic acid substituted porphyrin **TCPP** (Fig. 6). These porphyrins exhibit long-lived (>1 ns) π^* singlet excited states and only weak singlet/triplet mixing. They have an appropriate LUMO level that resides above the conduction band of the TiO₂ and a HOMO level that lies below the redox couple in the electrolyte solution, required for charge separation at the SC/dye/electrolyte surface. The relative LUMO and HOMO energy levels have been estimated for a range of dyes including **TCPP**, **Zn-TCPP** and **N3** bound to TiO₂ using a new UV photoemission yield technique [21]. Both Grätzel and co-workers [22] and Fox and co-workers [23] have

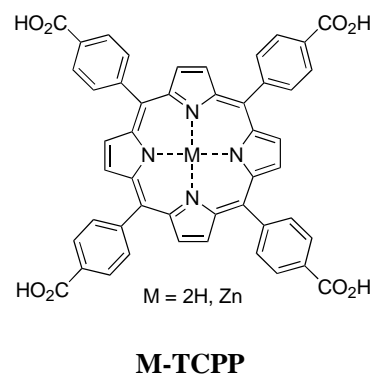


Fig. 6. Tetrakis(4-carboxyphenyl)porphyrins (**M-TCPP**).

reported efficient charge injection from the excited state of **Zn-TCPP** into the conduction band of TiO₂ (IPCE_{Soret} = 42%, IPCE_{Q band} = 8–10%) and (IPCE_{Soret} = 9.5%, $I_{sc} \approx 2.5 \mu\text{A cm}^{-2}$), respectively, however no AM1.5 normalised cell efficiencies were stated. Boschloo and Goossens [24] photosensitised TiO₂ with **Zn-TCPP**, giving a low η of 1.1% (IPCE_{Soret} = 40%, IPCE_{Q band} \approx 10–16%, V_{oc} = 0.36 V, I_{sc} = 0.85 mA cm^{-2}). A more recent and promising result is that from Cherian and Wamser [25] whose **TCPP**-based TiO₂ photovoltaic cells gave good solar-energy conversion efficiencies under AM1.5 conditions (η = 3.5%, fill factor of 62%, IPCE_{Soret} = 55%, IPCE_{Q band} = 25–45%, V_{oc} = 485 mV, I_{sc} = 6 mA cm^{-2}). To date this is the best-reported value for a porphyrin PEC, and was achieved using deoxycholic acid (DCA) as a co-adsorbate. Wamser [26] have also reported a solid state based Grätzel cell, that uses aminophenyltricarboxyphenylporphyrin dye **TC₃APP** with an aniline gel-based electrolyte system, giving an η value of 0.8%.

Recently, Durrant and co-workers [27] compared the electron injection and charge recombination of **N3**, free-base **TCPP** and **Zn-TCPP** on TiO₂. Their studies show that these three dyes have almost indistinguishable electron injection and recombination kinetics. They state that the high efficiency reported for **N3** dye probably originates from differences in the rate of electron transfer to the dye cation from the iodide redox couple used in these devices. It is also possible that the lower efficiency of porphyrin sensitizers results from the increased probability of exciton annihilation from close porphyrin proximity. Porphyrins have an inherent tendency to aggregate [28], and at high dye coverage, dipole/dipole interactions are expected to allow rapid migration of the excited state between neighbouring dyes, increasing the probability of exciton annihilation.

Odobel et al. [29] are currently investigating a range of regioisomers of *meso*-substituted phosphonic acid functionalised porphyrins. They claim that the nature of the functional group has little impact on the DSSC performance, but the position of substitution (*meta*, *para*) has a greater influence. They have also compared derivatives containing carboxylic acid **TCPP**, sulphonic acid **TSPP** and **TPP** in

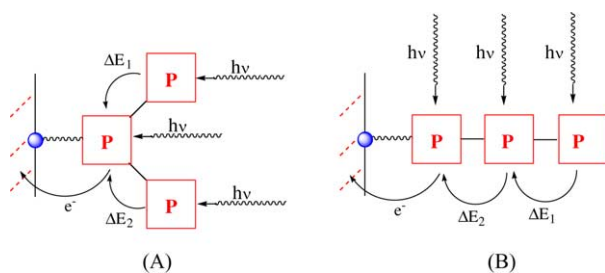


Fig. 7. Branched **A** and linear **B** approaches to chromophore antenna systems.

the DSSC [30]. Their results indicate that the binding state and the amount of dye adsorbed are all important factors in DSSC performance.

Another approach to harvesting photons more efficiently by chromophores is to construct arrays of chromophores, “molecular antennae”, and attach them to SCs or metals [20,31]. By linking a graded series of chromophores in a branched **A** or linear **B** array or assembly, using appropriate spacers or bridging units, the higher energy chromophore transfers excitation energy to the lowest energy chromophore, which injects charge into the acceptor surface (Fig. 7). The efficiency of the intramolecular energy and electron transfer processes in antennae assemblies will depend on the extent of electronic coupling between chromophores. This will be modulated both by the bridge and the spatial orientation of individual chromophoric units. While any type of chemical forces could, in principle, be used to link molecular components, covalent bonding via an appropriate bridging group seems to be the best choice for a stable antennae system. The obvious requirements for an antenna are, an efficient antennae effect channelling the absorbed energy towards the surface component, and the capability of the excited molecular component bound to the SC or metal surface to inject electrons into the conduction band (Fig. 7).

There are significant energy-related problems associated with multi-component chromophore systems. If a finite energy demand (ΔE) exists for each parallel transfer step, a branch design (Fig. 7, **A**), utilising parallel energy processes ($\Delta E_{\text{total}} = (1/\Delta E_1 + 1/\Delta E_2)^{-1}$), should be more energy efficient than the linear design (Fig. 7, **B**) where all processes

are in series and energy demands are additive ($\Delta E_{\text{total}} = \Delta E_1 + \Delta E_2$). In the case of the highly branched antenna system, however, a much larger surface area on the SC will be occupied by each bound chromophoric array, compared to that of a linear array sensitizer. At saturation coverage, this would reduce any gain achieved from the antennae effect. From this point of view, the linear design would be superior to the branched one. These arguments, however, should be treated with caution as the SC surface available for absorption is far from being an idealised flat surface. In nanocrystalline photoanodes, an extremely rough surface is present, mostly made up of pores and cavities with nanometer dimensions. As such, the fitting requirements of arrays in pores may be the ultimate determining condition.

TiO₂ and SnO₂ have also been sensitised by collinear porphyrin dyad systems. Koehorst et al. [32] constructed a cell from Zn/free-base diporphyrin heterodimers adsorbed on TiO₂ (Fig. 8). Surprisingly both diporphyrins give similar monochromatic IPCE results (IPCE_{430nm} = 3%, I_{sc} = 10 mA cm⁻²), even though energy transfer and electron transfer in monolayers of **Dimer A** are *consecutive* whereas in monolayers of **Dimer B** both processes are *competitive*. It was suggested that the similar IPCE values are the result of a favourable light collecting antennae effect.

The photosensitization of SnO₂ with a Zn/free-base diporphyrin dyad, P_{Zn}-P, and separately with the monomers P and P_{Zn} has been investigated by Sereno and co-workers [33–36]. Maximum IPCE values of ≈6, 32 and 11% were obtained at the Soret band of ITO/SnO₂/P_{Zn}, ITO/SnO₂/P and ITO/SnO₂/P_{Zn}-P, respectively. The photocurrent efficiency of the dyad P_{Zn}-P is low compared to P. This is to be expected as there is no control over which porphyrin of the dyad is bound to the surface. A number of other dyads, triads and tetrads have recently been synthesised by Lindsey and co-workers [37] but solar cell results are as yet not available.

Investigations into the efficiency of porphyrins linked to a surface through the β-pyrrolic position of the macrocycle are rare. The use of natural porphyrins, zinc and antimony metallo-uroporphyrins **M-UP** (Fig. 9) as photosensitisers were investigated by Kalyanasundaram et al. [38] They obtained monochromatic IPCE values of 4.5% at

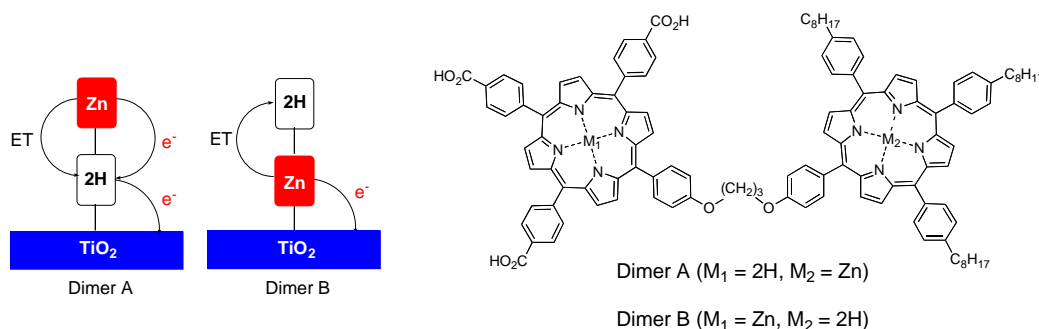
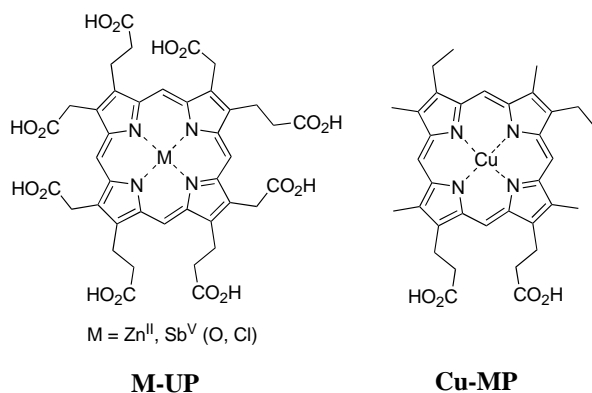
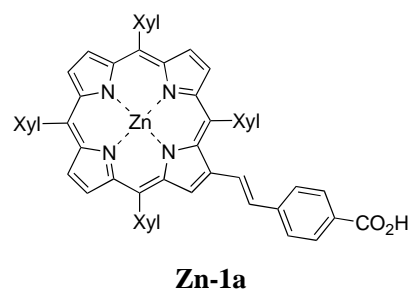


Fig. 8. Heterodimers **A** and **B** on TiO₂ [32].

Fig. 9. Uroporphyrin **M-UP** and Cu-*meso*-porphyrin **Cu-MP**.

540 nm for the zinc-uroporphyrin **Zn-UP** (Q(1, 0) band of **Zn-UP**). Grätzel and his group have also studied a number of natural metallochlorophyll derivatives and related natural metallo-*meso*-porphyrins **M-MP** (Fig. 9) for the photosensitisation of TiO₂ solar cells [39,40]. These cells showed efficient sensitisation of TiO₂, with near unity quantum efficiency of charge injection for Soret peak illumination of Cu-*meso*-porphyrin **Cu-MP**. The η value of the cell was 2.6%. They concluded that free carboxyl groups are important for adsorption, however, conjugation of the carboxyl groups to the π electron system of the chromophore is not necessary for efficient electron transfer with a linker of this length. The study also revealed a strong dependence on the type of solvent and type of co-adsorbates.

Studies of electron transfer in porphyrin–quinone (donor–acceptor) systems show that porphyrin ring oxidation is eas-

Fig. 10. TXP benzoic acid derivative **Zn-1a**.

ier for β -substituted porphyrins than for *meso*-substituted ones [41]. This may also facilitate better electron transfer in PEC applications. In addition, in *meso*-substituted porphyrins, where orthogonal phenyl rings dominate, conjugation from the macrocycle to the binding group is not possible. Conjugation, however, can occur through a styryl β -pyrrolic linker [42,43], and our research has focused around the synthesis of porphyrin systems based on the use of β -pyrrolic substitution with tetraarylporphyrin (TAP) phosphonium salts [44]. This has given rise to dependable synthetic routes to a range of conjugated β -pyrrolic substituted carboxylic acid functionalised porphyrins, from discrete mono-substituted derivatives, to larger multi-porphyrin arrays, based on a building block approach [45]. Using this approach, a variety of the discrete mono β -substituted TAP benzoic acid porphyrins analogues of **Zn-1a** (Fig. 10) were synthesised and their light harvesting ability investigated.

In addition, in order to investigate the advantages that could be gained from an antennae effect, we systematically

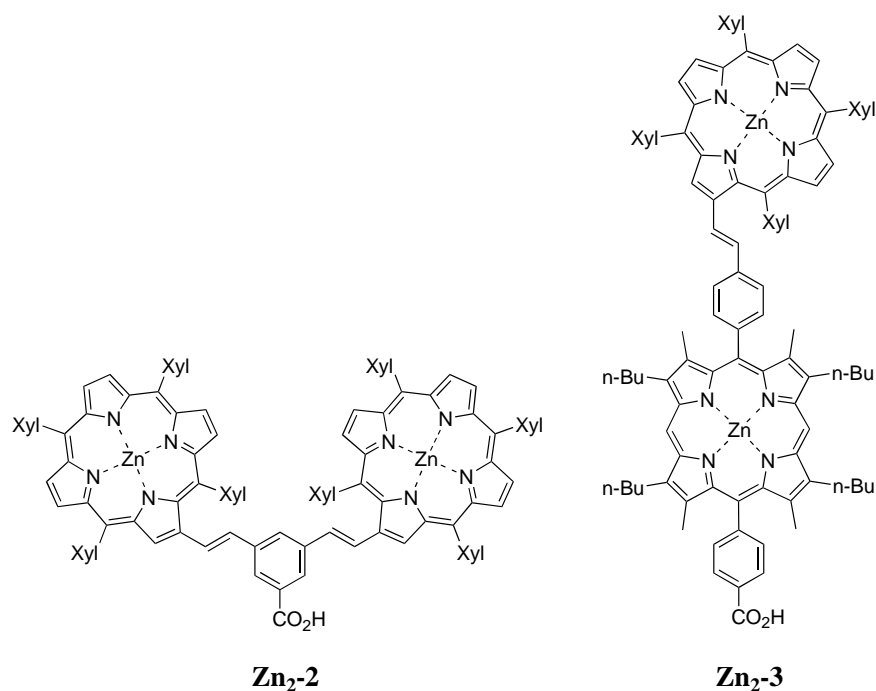


Fig. 11. Branched and linear porphyrin dimers.

synthesised branched and linear dimeric-porphyrin antenna systems (Fig. 11) and assessed their light harvesting efficiency attached to nanocrystalline TiO_2 .

Furthermore, an alternative approach to array systems was undertaken by constructing them from porphyrins already containing the acid functionality. This was achieved with the development of a new “sticky” TAP phosphonium salt based on **T3CPP** (see Table 3). This second array approach differs in that arrays were constructed through a mixture of β -pyrrolic and *meso*-linkers, therefore binding to the TiO_2

surface occurs through multiple *meso*-binding groups and chromophore sites. Using this approach, a series of diporphyrins, triporphyrins and pentaporphyrins, known here as ‘sticky’ porphyrins, as shown in Fig. 12, were synthesised and evaluated.

While many factors are known to determine the performance of a PEC, a complete quantitative comparison of the porphyrin dyes would have been extremely time consuming. The purpose of the present study was, therefore, to establish a qualitative comparison and evaluation of the effectiveness

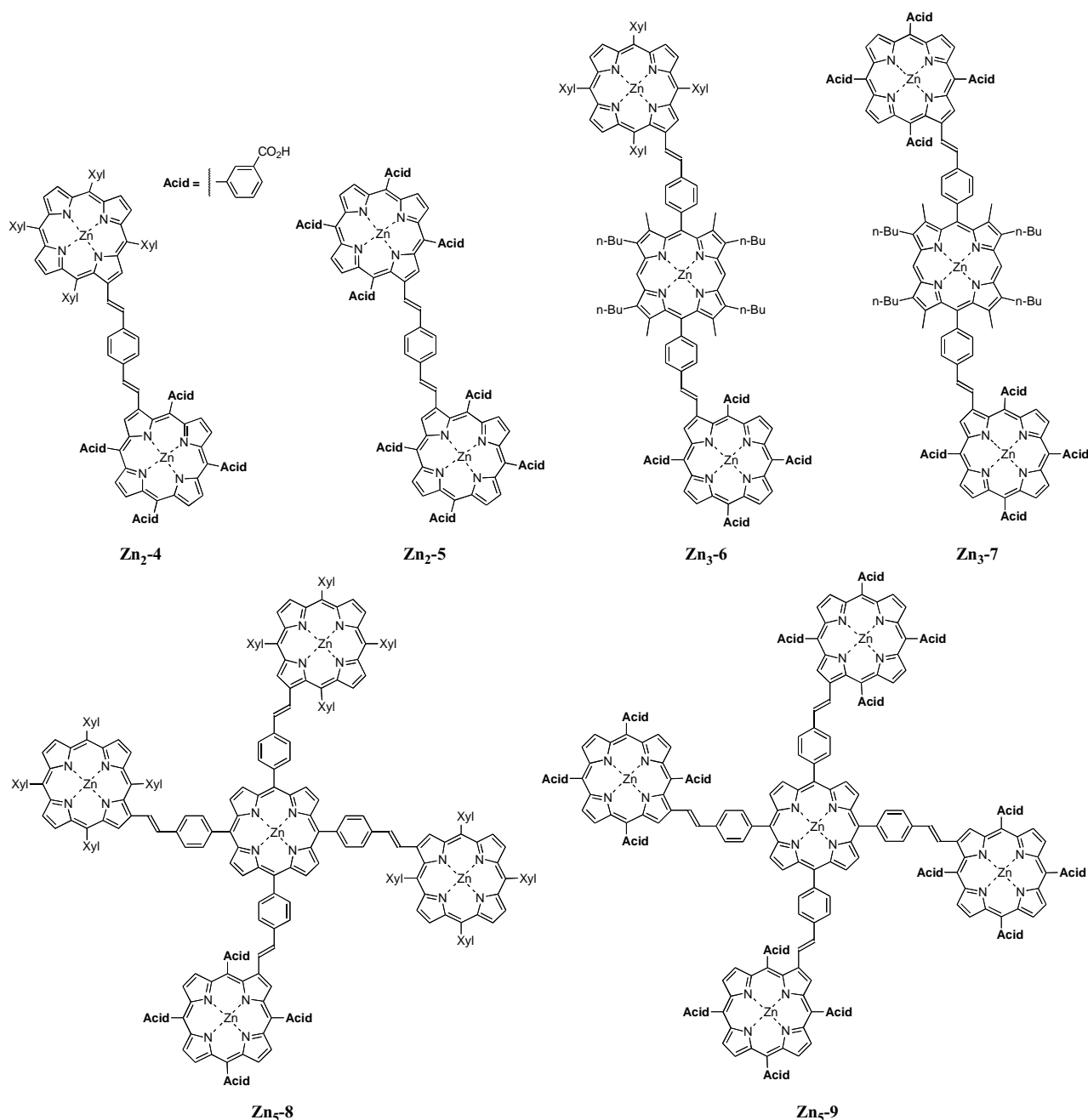


Fig. 12. ‘Sticky’ porphyrin arrays.

of these dyes as light sensitisers in a PEC cell. Initially the dye **Zn-1a** was used to optimise the PEC conditions and performance.

2. Experimental

2.1. Porphyrin syntheses

The syntheses of the porphyrins used in this study (to be published elsewhere [46]), were achieved by combining a mixture of porphyrin Wittig chemistries developed in these laboratories using the appropriate functionalised aldehydes, integrated with classical porphyrin forming condensation reactions. The key to the efficient syntheses of the acid derivatives was to synthesise the parent compounds as esters derivatives, followed by hydrolysis as the last step to the desired acids.

2.2. The test cell

We set out to establish equipment and procedures to develop a semi-quantitative dye screening protocol that would provide enough information to allow us to identify promising dyes. The whole testing regime needed to be simple and allow the performance of many dye samples to be quickly evaluated. A Grätzel cell was specifically designed and constructed for this purpose. Such a cell output is dependent on many factors other than the dye itself. In particular, it depends strongly on the thickness and quality of the TiO₂ plates¹ and electrolyte composition used. In order to counter these effects, a dye standard, generally the TXP derivative **Zn-1a** and later the TPP derivative **Zn-1b**, was used. The apparatus consisted simply of a 50 W halogen bulb [47] light source positioned above an X–Y–Z microscope stage, and connected to a regulated power supply. A Darlington Phototransistor sensor was fabricated into a calibration sensor by imbedding it in an epoxy resin case. This was used prior to every test to ensure that the light intensity ($\approx 100 \text{ mW cm}^{-2}$) was consistent. A cell holder was also fabricated to hold dye-coated TiO₂ coated conducting glass, which incorporated a light spring to hold a solid Pt counter electrode against the TiO₂ layer. The final apparatus, cell set-up, and following testing procedures allowed us to quickly and qualitatively screen a large number of samples.

2.3. Testing procedure

2.3.1. TiO₂ electrode preparation

Sections (10 mm \times 15 mm) of TiO₂ coated ITO glass supplied by Sustainable Technologies Australia Ltd (STA) were prepared using a cutting guide. One edge of the TiO₂

layer was then scraped back for an electrode contact point, to give a 10 mm \times 10 mm section. Later plates were supplied screen-printed as 7 mm \times 9 mm TiO₂ sections. The TiO₂ plates were then pre-treated by washing with ethanol (30 min), hexane (30 min), Milli-Q-water (30 min) and then rinsed with ethanol again prior to drying.

2.3.2. Dye adsorption

Prior to dye adsorption, the plates were fired at 490 °C for 30 min and then immersed in the dye solution while still warm. The plates were immersed in sealed containers of dye solution ($2 \times 10^{-4} \text{ M}$) for overnight adsorption (12–20 h) prior to testing. UV-Vis analysis of dye adsorption indicated that complete adsorption usually occurs in 5 h. Most dye adsorptions were carried out using about 10 ml per 1.0 cm² of TiO₂ area. The TiO₂ plates were removed from the dye solution directly before testing and the excess solvent removed by blotting on lint-free tissue paper and then drying under high vacuum for 5 min prior to cell assembly in the cell holder.

2.3.3. Platinum counter electrode preparation

The Pt counter electrode (13 mm \times 12 mm) was stored in ethanol until required. The cell side was polished by rubbing on lint-free paper wetted with acetone on a flat glass surface prior to each test run.

2.3.4. Cell assembly and electrolyte introduction

Prior and during assembly of the cell, the cell holder electrodes were short-circuited (to prevent any damaging V_{oc} conditions within the cell before testing). Following the clamping of the dyed TiO₂ electrode into the cell holder, the Pt counter electrode was placed against the TiO₂ layer while releasing the counter electrode contact support onto the Pt plate. Electrolyte was then introduced by capillary action into the cell between the two cell electrode surfaces and any excess electrolyte removed with a paper towel. Electrolytes used in this study included; **Electrolyte E** (0.5 M NaI, 0.05 M I₂, in glutaronitrile), **Electrolyte G** (0.5 M NaI, 0.05 M I₂, 4-*t*-butylpyridine (0.01 mol l^{-1}) in glutaronitrile), **Electrolyte 1376** (0.6 M, butylmethyylimidazolium iodide, BMII), 0.05 M I₂, LiI 0.1 M, 0.5 M *tert*-butylpyridine, 1:1 acetonitrile:valeronitrile).

2.3.5. Calibration of light source and testing

The bulb assembly required a 15-min warm up before testing, to stabilise any thermal drift. After calibration of the light source the assembled cell holder was connected up to a multimeter then placed into the testing rig, in a closed circuit current (I_{sc}) reading mode.

2.3.6. Data acquisition

The data collection system consisted of a Digitech Multimeter with a PC RS232C interface. I_{sc} data was recorded automatically every 30 s, and V_{oc} readings were performed for 5 s (V_{oc} reading times were kept short to eliminate any

¹ Different batches of TiO₂ plates are identified by a plate number, e.g. PA1.

damaging open circuit conditions). V_{oc} readings were generally taken after either a steady state (SS) or a maximum I_{sc} value was observed. All I_{sc} values recorded were corrected to mA cm^{-2} by accurately measuring the TiO_2 area with Vernier calipers after testing.

2.3.7. Results analysis and errors

In general, the protocol for the final screening of porphyrins involved the fabrication and testing of three to four separate cells for each compound. Any cell results that appeared as outliers were discarded; if this was a result of poor cell mechanics (i.e. short-circuiting between electrodes or damaged TiO_2 layer) generally a low V_{oc} resulted, allowing a confident exclusion of this result. Generally maximum I_{sc} values are used. Normally ‘standard deviations’ did not exceed 8% in I_{sc} . Therefore, the errors in I_{sc} measurements are conservatively displayed as 10% errors in the following data. V_{oc} errors rarely exceed 2% and are not displayed in the results.

3. Results and discussion

The Wittig-based building block approach to the development of porphyrin arrays and the concomitant introduction of surface binding functionality has provided us with an unprecedented opportunity to investigate a wide variety of electronic and structural features that could have a dramatic effect on the light harvesting ability of porphyrins in PECs. Therefore, we have chosen to do this qualitatively so as to provide a rapid analysis of as wide a variety of parameters as possible. The most promising dyes would then be subjected to a more rigorous study.

Along with the type of solvent and concentration used for the adsorption process, a variety of general porphyrin physical and structural features were first investigated, these being the type of metalloporphyrin that would give the best cell performance, and the form of the acid moiety (i.e. salt or free acid). Comparisons were then made with a range of

Table 1
Salts of **Zn-1a**

Dye	I_{sc} (mA cm^{-2})	V_{oc} (mV)
Zn-1a	0.73 (7)	478
Zn-1a(Na)	0.27 (3)	388
Zn-1a(TBA)	0.066 (7)	292

Electrolyte E, PA1 Plate.

mono *meso*-benzoic acid porphyrin dyes, followed by evaluation of the proposed array systems. Finally further optimisation of the **Zn-1a** based cell was undertaken, exploring the effect of different, *o,m,p*-regioisomers, steric aryl groups, electrolytes, binding groups and the importance of linker conjugation.

3.1. Initial test cell and chromophore optimisation

The solvent used to prepare the dye solutions had a significant effect on the cell performance (Fig. 13). Clearly the solvent that gave the best cell performance for **Zn-1a** is THF and this solvent was used for all the dye comparisons. Dye concentration during the adsorption process is also important to cell performance. For the **Zn-1a** dye, the optimum concentration appears to be somewhere between 10^{-4} and 10^{-5} M, and a standard dye concentration of 2×10^{-4} M was chosen.

Also, in order to ascertain whether the free carboxylic acid or a salt is best for cell efficiency, the sodium **Zn-1a(Na)** and the tetrabutylammonium **Zn-1a(TBA)** salt derivatives of the free acid **Zn-1a** were synthesised and tested (Table 1). As the free acid form **Zn-1a** gave superior cell performance, the subsequent acids were tested in their free acid form only.

It is also well known [48] that the coordination of metal ions in the porphyrin core has an effect on the life times of the excited electronic states, which, in turn, can influence the electron transfer process between the chromophore and the conduction bands of the TiO_2 . In addition, metallation affects the chemical and physical properties of porphyrins. The cell performance of Zn(II),

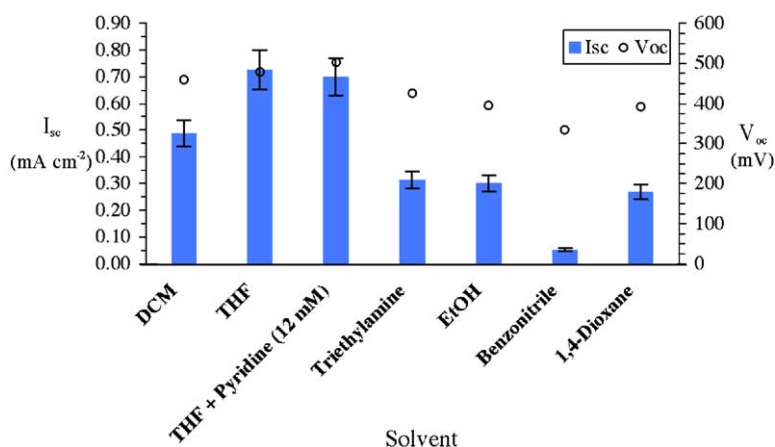
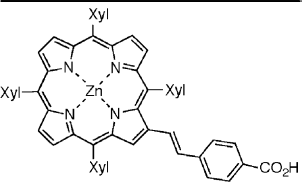
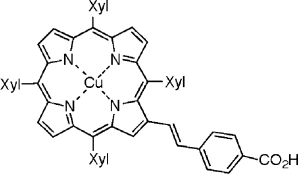
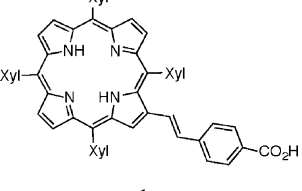


Fig. 13. Adsorption solvent influence for **Zn-1a** (Electrolyte E, PA1 Plates, 10^{-5} M).

Table 2
Effect of metallation of **1a** on cell performance

Dye	I_{sc} (mA cm ⁻²)	V_{oc} (mV)
 <p>Zn-1a</p>	1.2 (1)	459
 <p>Cu-1a</p>	0.61 (6)	460
 <p>1a</p>	0.018 (2)	198

Electrolyte E (0.5 M NaI, 0.05 M I₂, in glutaronitrile), PA2 Plate.

Cu(II) and the free-base derivatives of **1a** are summarised in Table 2.

The Zn(II) derivative **Zn-1a** performs better than the Cu(II) **Cu-1a** and the free-base species **1a**. Both **Zn-1a** and **Cu-1a** cells developed a SS behaviour in their I_{sc} values and showed good recovery in I_{sc} after a V_{oc} condition. Cu(II) porphyrins are known to have shorter lived excited states compared to the zinc porphyrins, but they are inherently more stable [49]. Although the **Cu-1a** cell performance was half of the **Zn-1a** I_{sc} value, the results suggest that Cu(II) porphyrins may be useful where long term stability of the chromophores is required in solar cells. Based on these results and the ease of synthesis and characterisation of Zn(II) porphyrins, all subsequent chromophores were synthesised and tested as Zn(II) metallo derivatives.

3.2. Comparison of β - and meso-substituted monoporphyrin carboxylic acids

The β -substituted **Zn-1a** carboxylic acid and a range of Zn(II) meso-benzoic acid monoporphyrins were tested in the Grätzel cell (see Table 3).

The β -substituted **Zn-1a** monoacid, performed considerably better than all the meso-substituted porphyrin dyes. The superior performance of **Zn-1a** suggests that the mode of binding is an important factor in determining cell performance. The porphyrins could lie flat on or edgewise to the SC surface. Edgewise binding would allow a significantly

Table 3
Mono porphyrin acids

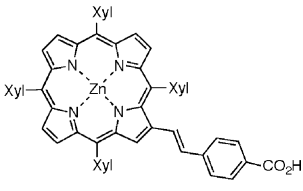
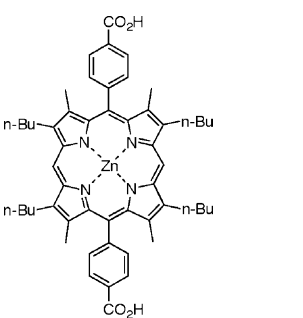
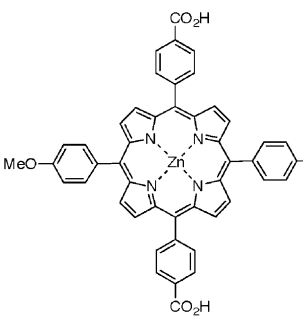
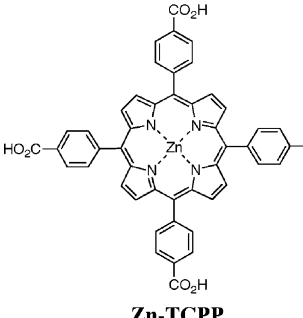
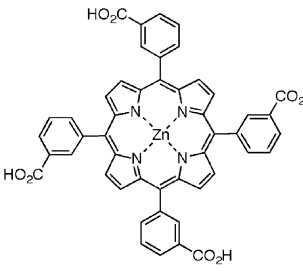
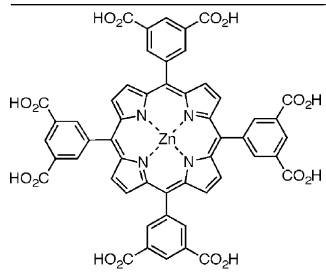
Dye	I_{sc} (mA cm ⁻²)	V_{oc} (mV)
 <p>Zn-1a</p>	0.84 (8)	453
 <p>Zn-BCPP</p>	0.018 (2)	118
 <p>Zn-BCMPP</p>	0.20 (2)	299
 <p>Zn-TCPP</p>	0.079 (8)	204
 <p>Zn-T3CPP</p>	0.41 (4)	363

Table 3 (Continued)

Dye	I_{sc} (mA cm ⁻²)	V_{oc} (mV)
 <p>Zn-T3,5CPP</p>	0.15 (1)	285

Electrolyte E, PD1 Plate.

higher dye concentration on the highly uneven, porous TiO₂ surface than flat binding. It is likely that **Zn-1a** binds predominantly edgewise (Fig. 14, **1a**), given the single binding functionality. In contrast, it might be anticipated that a larger number of carboxylic functionalities might force the porphyrin to lie flat on the surface. Of the tetra-*meso*-acid porphyrins, **Zn-T3CPP**, **Zn-TCPP** and **Zn-T3,5CPP**, the *meta*-substituted monoporphyrin **Zn-T3CPP** gave significantly higher I_{sc} and V_{oc} results, with an I_{sc} value four-fold higher than the *para*-acid derivative **Zn-TCPP**, and 50% of **Zn-1a**. Simple modelling of the tetra acids (Fig. 14) clearly demonstrates that while **T3CPP** could lie flat on the surface with all four acid groups available for binding, this would not be the case for **TCPP**. Indeed, Cherian and Wamser have concluded that **TCPP** itself likely binds to TiO₂ in “a variety of different adsorption modes including multilayers” rather than a fully flat geometry [25]. Therefore, the predominant factor for the improved efficiency of **Zn-1a** over **Zn-TCPP** could be the improved charge transfer through the fully conjugated system, along with a higher surface area coverage by this possibly edgewise-bound porphyrin. The nearly orthogonal electronically decoupled *meso*-benzoic acids may limit charge injection from **Zn-TCPP**. In contrast, if the *meta*-**T3CPP** can adopt a fully flat binding mode, this might allow more efficient direct charge injection from the por-

phyrin to the SC surface, accounting for the higher performance of this tetra acid.

It was also noted that generally the low I_{sc} values of all the multiacid porphyrins were accompanied by the observation of faint dye colourations and shadowing on the TiO₂ surface after removal from the dye solution, indicating poor binding or low surface coverage. The weak binding of these acids is surprising considering the number of carboxylic acid groups (4–8) present on these molecules. However, given the potentially flatter binding modality of the multiacid porphyrins, lower surface coverage is to be expected and the rough, nanocrystalline TiO₂ may not be the optimal surface for flat binding.

In addition, Odobel et al. [29] have shown that the position of substitution (*meta*, *para*) of the binding functionality has a significant influence on the sensitisation efficiency of porphyrins. It is apparent that this is indeed the case here, with the porphyrins containing *meta* binding functionality showing superior cell performance to those with *para* binding functionality. This may again be a result of the surface binding modality.

Finally, of the *meso*-substituted dyes, the I_{sc} for **Zn-BCMPP** is an order of magnitude larger than that for **Zn-BCPP**, and 24% of the **Zn-1a** I_{sc} value. The higher I_{sc} value for **Zn-BCMPP** over **Zn-BCPP** may possibly result from the introduction of electron donating methoxyphenyl groups to the porphyrin periphery.

3.3. Array porphyrins

3.3.1. “Branched” and “linear” arrays

Clearly from Table 4, it can be seen that **Zn-1a** outperforms both array systems. The “branched” diporphyrin **Zn₂-2** and the “linear” diporphyrin **Zn₂-3**, gave similar, low SS I_{sc} values (11% of **Zn-1a**, Table 4). Adsorption of these dyes resulted in a pale TiO₂ colouring, accompanied by significant shadowing of the TiO₂ layer after removal from the dye solutions. Rinsing of a dye-bound TiO₂ plate with THF resulted in removal of most of the dye. This is consistent with weak surface adhesion. These cells were slow to reach a SS I_{sc} (>100 min). This may have resulted from slow redistribu-

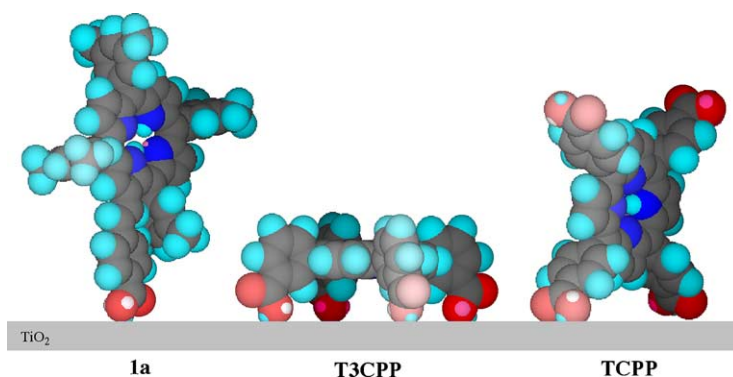
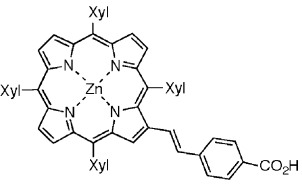
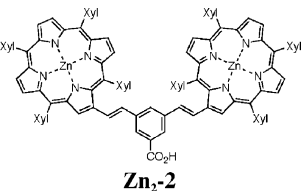
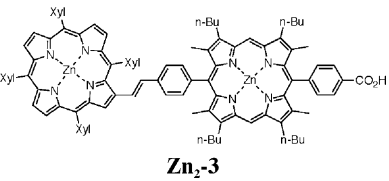
Fig. 14. Computer-generated CPK models of **1a**, **T3CPP** and **TCPP**.

Table 4
Branched and linear porphyrin arrays in the TiO₂ PEC

Dye	I_{sc} (mA cm ⁻²)	V_{oc} (mV)
 <p>Zn-1a</p>	0.84 (8)	453
 <p>Zn₂-2</p>	0.11 (1)	307
 <p>Zn₂-3</p>	0.089 (9)	244

Electrolyte E, PD1 Plate.

tion of the porphyrin molecules within the TiO₂ layer and/or with the electrolyte. Clearly, these results do not allow the identification of a significant antennae effect for either of these array systems in this type of PEC. Their overall poor performance may ultimately be the result of poor binding.

3.3.2. “Sticky” porphyrin arrays

In contrast to the branched and linear arrays, the ‘sticky’ porphyrin arrays bind strongly to the TiO₂. Rinsing did not result in dye desorption and a dark green/brown TiO₂ surface was evident in all cases after removal from the dye solution. Yet here also the monoporphyrin **Zn-1a** outperforms these dyes, with no apparent antennae effect observed in spite of the strong binding.

The T3CPP based “sticky” array diporphyrins **Zn₂-4**, **Zn₂-5** and triporphyrins **Zn₃-6**, **Zn₃-7** revealed a similar trend in their I_{sc} values (Table 5). For each pair, the arrays with more acid groups gave the lower value. Since the arrays with the free TXP moieties (**Zn₂-4** and **Zn₃-6**) gave the highest outputs, this perhaps suggests that the porphyrin array is a better photosensitiser when it is not held too close to the surface, but tethered in close proximity. The triporphyrins cells did not reach SS, indicating poor current stability. The star shaped pentaporphyrins **Zn₅-8** and **Zn₅-9** gave similar I_{sc} results to those of the triporphyrins (Table 5). Since the triporphyrins and pentaporphyrins cells did not reach SS, only the maximum I_{sc} values are taken, and direct comparisons to those from SS cells cannot be made.

The observation that the I_{sc} values are considerably lower than that of **Zn-1a** supports the notion that it is advantageous

for the binding group and linker to be positioned through the β -pyrrolic of the porphyrin chromophore. It is also highly likely that the small porosity of the TiO₂ nanocrystalline layer may be preventing adsorption of these very bulky dyes.

3.4. *o,m,p*-Carboxylic acids

The effect on cell performance by the acid regioisomers of **Zn-1a** was investigated and is displayed in Table 6. The varying steric and electronic effects of these isomers should affect the binding ability of the dye and the orientation and proximity of the porphyrin core to the TiO₂ surface.

It is clear that the *para*-Zn(II) metalloporphyrin acid **Zn-1a** performed the best, with cell performance dropping off from *para*, *meta* to *ortho*. If the TAP group is electron donating (reducing the acidity) the *meta*-acid derivative might be expected to bind stronger due to greater electronic isolation. This is however not the case, and possibly suggests surface geometry of the porphyrin is more critical. The low I_{sc} value for the *ortho*-species **o-Zn-1a** is not unexpected, as a very light colour of porphyrin was observed on the TiO₂ surface after 10 h of adsorption, suggesting poor binding. Significant steric constraints on binding imposed by the *ortho*-acid group would be expected to hinder binding of this dye. The *meta*-diacid ZnTXP=Ph_m(CO₂H)₂ **m,m-Zn-1a** gave similar I_{sc} results to the mono *meta*-derivative **m-Zn-1a**. Strong shadowing was seen on the TiO₂ layer on removal from the dye solution again implying weak binding.

3.5. Arylporphyrin substituents (TPP versus TXP versus TBP)

It has been suggested that the lower efficiency of porphyrin sensitisers results from the increased probability of exciton annihilation from close porphyrin proximity, as a result of porphyrin aggregation. Aggregation can be significantly diminished by increasing the steric interactions between porphyrins through the attachment of bulky aryl substituents. It might be anticipated therefore, that if aggregation is a problem, then replacing the *meso*-aryl groups of **Zn-1a** with larger groups should improve cell performance.

The performance of PECs containing TXP and TBP derivatives (**Zn-1a** and **Zn-1c**) were found to be comparable but surprisingly the TPP **Zn-1b** derivative gave a significantly higher I_{sc} value (Table 7). A second set of cells were run at a later date using a new Electrolyte 1376 on different batch of TiO₂ plates. These results also showed no significant differences in I_{sc} between the TXP and TBP derivatives, the **Zn-1b** still being superior. It is tempting to infer from these results that closer porphyrin proximity enhances light harvesting on the SC surface. This might not be surprising given the nature of photosynthetic light harvesting complexes. However, the *meso*-aryl substituent significantly varies the electronic nature of the porphyrin and attached functionality, as we have observed through the

change in reactivity of various porphyrin styryl benzaldehydes [50]. Therefore, this improved performance may be entirely due to electronic tuning of the porphyrin orbitals to better interact with the TiO₂ conduction band. Nonetheless, it is not unreasonable to draw the conclusion from these observations that close proximity of porphyrins may not significantly diminish light harvesting.

Given the improved light harvesting performance of the TPP derivative **Zn-1b**, it was used as the new reference compound and the base porphyrin core in future porphyrin synthesis.

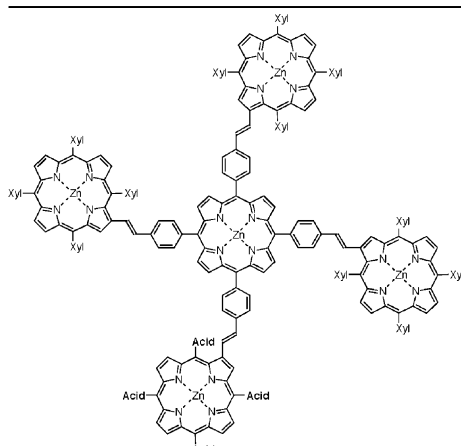
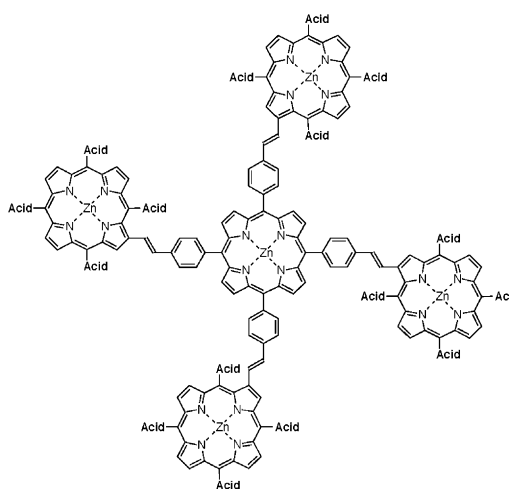
3.6. Electrolyte influence

The nature of the electrolyte has a significant impact on the cell performance (Table 8). As indicated in Table 2, it was observed that the current generated from the Cu(II) TXP derivative of **M-1a** was 50% less than that of the Zn(II) derivative when using **Electrolyte E** on PA2 plates. This is also the case with **Electrolyte 1376**, which gives superior performance for the Zn(II) TPP derivative **Zn-1b** (Table 8). Surprisingly, **Cu-1b** has a very small I_{sc} output in **Electrolyte 1376** yet still maintains a good V_{oc} . In **Electrolyte G**

Table 5
'Sticky' porphyrin arrays in the TiO₂ PEC

Dye	I_{sc} (mA cm ⁻²)	V_{oc} (mV)
<p>Zn-1a</p>	0.84 (8)	453
<p>Zn₂-4</p>	0.27 (3)	332
<p>Zn₂-5</p>	0.12 (1)	297
<p>Zn₃-6</p>	0.35 (4)	364
<p>Zn₃-7</p>	0.23 (2)	343

Table 5 (Continued)

Dye	I_{sc} (mA cm ⁻²)	V_{oc} (mV)
 <p>Zn₈-8</p>	0.26 (3)	349
 <p>Zn₈-9</p>	0.29 (3)	362

Electrolyte E, PD1 Plate.

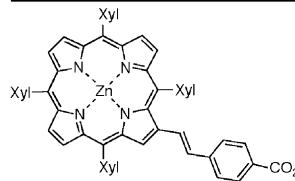
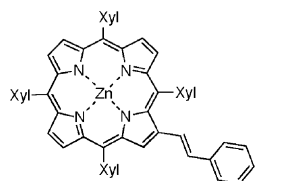
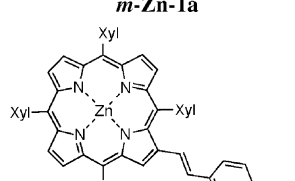
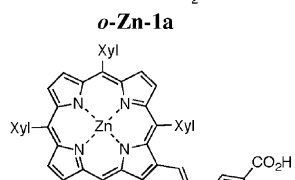
the overall cell performance is down, but there is no differentiation between the I_{sc} values of the two different metallo states.

3.7. Binding groups

It was apparent throughout these studies that the degree of binding of the porphyrin dyes to the SC surface was highly variable and undoubtedly reflected the electronic influence of the porphyrin moieties on the acid pK_a values. With the best dye **Zn-1b**, the dye-coated plates discoloured when they were rinsed in the adsorption solvent. In addition, on removal of the TiO₂ plates from the dye solution, a coloured patterning, known as “shadowing” was observed as the solvent front dried and carried dye across the TiO₂ surface. These observations suggest that **Zn-1b** is not strongly bound to the TiO₂. In contrast, the Ru dyes, such as **N3** and **Black Dye**, are known to bind strongly to TiO₂ and

are not removed by rinsing. This is presumably due to the greater acidity of the Ru dyes ($pK_a < 3.3$ [3,51]) compared to the TAP dye **Zn-1b**. While it has not been possible to determine the acid pK_a value for the latter, the porphyrin macrocycle is believed to be electron donating, leading to an acid pK_a greater than that for the parent benzoic acid ($pK_a = 4.2$). Thus, a stronger binding group might be expected to increase the cell performance and consequently the sulphonic acid **Zn-10** and phosphonic acid **Zn-11** (synthesised as the TBA salt) derivatives of **Zn-1b** were synthesised and tested. These new acids were not removed by rinsing and displayed no “shadowing” yet Table 9 shows that the carboxylic acid derived **Zn-1b** is significantly superior in SC sensitisation to either the sulphonic or phosphonic acid porphyrins. This tends to suggest that electronic coupling between the dye and TiO₂ surface through the binding group has an important role to play in the efficiency of light harvesting.

Table 6
o,m,p-Acids of **Zn-1a**

Dye	I_{sc} (mA cm ⁻²)	V_{oc} (mV)
 Zn-1a	0.87 (9)	422
 m-Zn-1a	0.67 (7)	436
 o-Zn-1a	0.0092 (9)	209
 m,m-Zn-1a	0.73 (7)	448

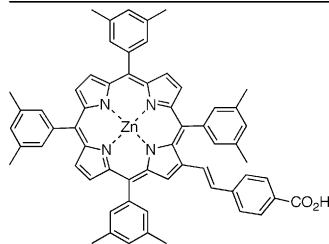
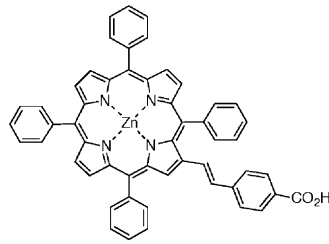
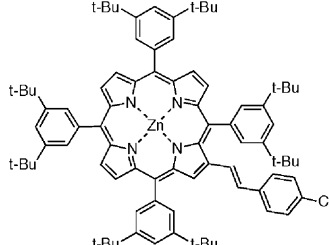
Electrolyte E, PB Plate.

3.8. Linker conjugation

One of the critical features of this work has been to demonstrate the value of the conjugative linkage between the porphyrin and the binding group. It was inferred from the results in Section 3.2 that it was this linkage that was responsible for the improved light harvesting performance of these β -pyrrolic substituted carboxylic acid functionalised porphyrins over the *meso*-aryl carboxylic acid functionalised porphyrins. Therefore, we not only prepared a variety of β -substituted carboxylic acid porphyrins with varying degrees of conjugation but also porphyrins with the conjugation removed (Fig. 15, **Zn-12** through to **Zn-18**).

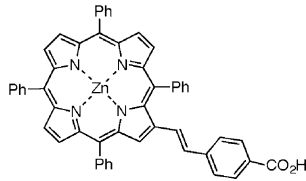
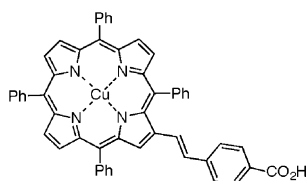
For the conjugated linkers, the number of double bonds, or the presence of the phenyl moiety, made no significant difference in overall cell performance. However, when the conjugation is interrupted, there is a significant fall in the cell performance. Both the reduced porphyrin of **Zn-1b**, **Zn-13** (ZnTPP-CH₂-CH₂-PhCOOH) and the phenyl acetic acid derivative **Zn-14** (ZnTPP-CH=CH-Ph-CH₂-COOH) gave consid-

Table 7
TXP (**Zn-1a**) vs. TPP (**Zn-1b**) vs. TBP (**Zn-1c**) derivatives

Dye	I_{sc} (mA cm ⁻²)	V_{oc} (mV)
 Zn-1a	0.73 (7)	423
 Zn-1b	1.1 (1)	434
 Zn-1c	0.64 (6)	403

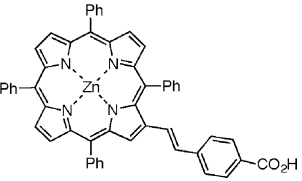
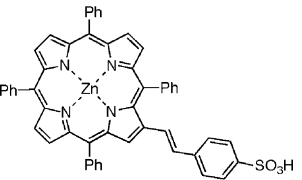
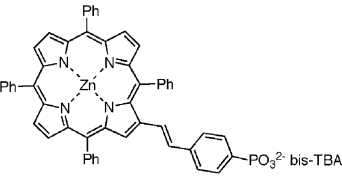
Electrolyte G, PD2 Plate.

Table 8
Electrolyte effect

Dye	Electrolyte	I_{sc} (mA cm ⁻²)	V_{oc} (mV)
 Zn-1b	G	3.1 (3)	442
	1376	5.3 (5)	597
 Cu-1b	G	3.1 (3)	505
	1376	0.054 (5)	505

Electrolyte G (0.5 M NaI, 0.05 M I₂, 4-*t*-butylpyridine (0.01 mol l⁻¹) in glutaronitrile), **Electrolyte 1376** (0.6 M, butyl-methyl-imidazolium iodide, BMII), 0.05 M I₂, LiI 0.1 M, 0.5 M *tert*-butylpyridine, 1:1 acetonitrile:valeronitrile) (PE Plate).

Table 9
Carboxylic vs. sulphonic vs. phosphonic acid binding groups

Dye	I_{sc} (mA cm ⁻²)	V_{oc} (mV)
 Zn-1b	5.2 (5)	597
 Zn-10	0.27 (3)	364
 Zn-11	0.21 (2)	410

Electrolyte 1376, Plate PE.

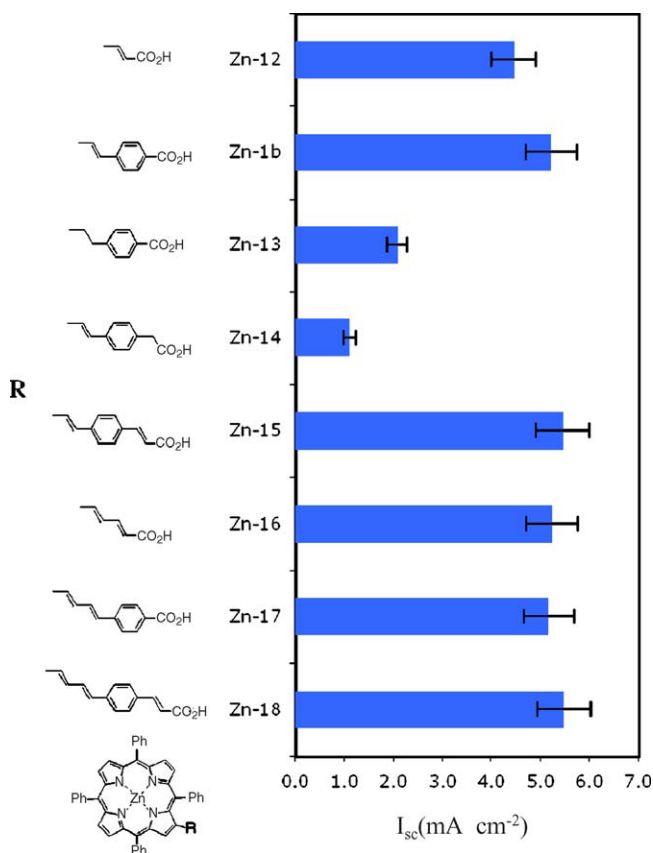


Fig. 15. Linker conjugation (Electrolyte 1376, PE Plate, V_{oc} vary from 500 to 600 mV).

erably lower I_{sc} values. Therefore, it appears clear that conjugation of the binding functionality to the porphyrin core significantly enhances solar cell performance.

3.9. Quantitative Grätzel cell results

The value of this approach to the screening of porphyrin dyes for PECs has been confirmed with independent quantitative testing of the best performing porphyrin dye **Zn-1b** in Professor Grätzel's laboratories at the Swiss Federal Institute of Technology (EPFL, Lausanne). **Zn-1b** gave a η of 4.24% (IPCE_{max} = 80%, I_{sc} = 9 mA cm⁻², V_{oc} = 654 mV, FF = 0.72) under AM1.5 conditions using **Electrolyte 1376**.² This value is better than the best-reported literature value of η = 3.5% for a **TCPP** TiO₂-dyed PEC [25].³

4. Conclusion

The successful development of a rapid screening of the efficiency of porphyrin dyes in nanocrystalline TiO₂ Grätzel cells has allowed the evaluation of a wide variety of functionalised porphyrin monomers and arrays, as well as a significant number of the structural and electronic parameters that influence light harvesting efficiency. We have shown that β -substituted porphyrin styryl carboxylic acids are superior to *meso*-aryl porphyrin carboxylic acids as light harvesters. Although this work does not allow an easy rationalisation of this difference, it is clear that surface orientation, electronic communication and the electronic nature of the porphyrin all profoundly affect its light harvesting ability. This study opens the way for a more in depth investigation of these factors. Zn(II) metalloporphyrin **Zn-1b** has been shown to be the most efficient porphyrin photosensitiser tested to date. This dye has an efficiency of η = 4.2%, which is an encouraging result for a porphyrin dye, and it offers potential for porphyrins as alternatives to Ru-based dyes in the DSSC. The results also suggest that Cu(II) porphyrins may be worth pursuing in future where long term stability of the chromophores is required in solar cells, although the choice of electrolyte is critical in this regard. Although sulphonic and phosphonic acid groups did offer stronger binding, they do not aid cell performance. Other metals (i.e. Mg, Ru, etc.) have yet to be assessed. It has been found that the adsorption solvent choice, electrolyte composition, and dye concentrations are all critical to cell performance, and should all be optimised for each dye in future studies. Finally, we have also shown that single porphyrin dyes are generally more efficient than a variety of porphyrin arrays. This surprising result may reflect more on the size and poor surface adsorp-

² TiO₂ electrodes of 6–7 μ m thick were used, prepared from 16 nm anatase TiO₂ paste (prepared by hydrolysis of titanium(IV)isopropoxide) deposited on to fluorine-doped stannic oxide glass (Tec-15, USA, 12–15 Ω) by screen printing.

³ See Note added in proof.

tion of the arrays than their ability to act as light harvesting antennae.

Note added in proof

Following submission of this manuscript, more detailed studies of Grätzel cells containing the *p*-styrylporphyrins **Zn-1a** and **Zn-1b** have led to a higher η of 4.80% (IPCE_{max} = 75%, I_{sc} = 9.7 mA cm⁻², V_{oc} = 660 mV, FF = 0.75). Md. K. Nazeeruddin, R. Humphry-Baker, D.L. Officer, W.M. Campbell, A.K. Burrell, M. Grätzel, Langmuir (2004), in press.

Acknowledgements

The authors wish to thank Dr. K. Nazeeruddin and Professor Michael Grätzel for the quantitative testing of porphyrin dyes. This research was supported by the New Zealand Foundation for Research, Science and Technology New Economy Research Fund contracts MAUX0014 and MAUX0202.

References

- [1] H. Arakawa, K. Hara, Mol. Supramol. Photochem. 10 (2003) 123.
- [2] A. Hagfeldt, M. Grätzel, Acc. Chem. Res. 33 (2000) 269.
- [3] M.K. Nazeeruddin, P. Pechy, T. Renouard, S.M. Zakeeruddin, R. Humphry-Baker, P. Comte, P. Liska, L. Cevey, E. Costa, V. Shklover, L. Spiccia, G.B. Deacon, C.A. Bignozzi, M. Grätzel, J. Am. Chem. Soc. 123 (2001) 1613.
- [4] M. Nazeeruddin, A. Kay, I. Rodicio, R. Humphry-Baker, E. Muller, P. Liska, N. Vlachopoulos, M. Grätzel, J. Am. Chem. Soc. 115 (1993) 6382.
- [5] H. Deng, Y. Zhou, H. Mao, Z. Lu, Synth. Met. 92 (1998) 269.
- [6] T.A. Hiemer, S.T. D'Arcangelis, F. Farzad, J.M. Stipkala, G. Meyer, J. Inorg. Chem. 35 (1996) 5319.
- [7] B. Burfeindt, T. Hannappel, W. Störck, F. Willig, J. Phys. Chem. 100 (1996) 16463.
- [8] J. Moser, M. Grätzel, J. Am. Chem. Soc. 106 (1984) 6557.
- [9] R. Abe, K. Hara, K. Sayama, K. Domen, H. Arakawa, J. Photochem. Photobiol. A 137 (2000) 63.
- [10] K. Sayama, M. Sugino, H. Sugihara, Y. Abe, H. Arakawa, Chem. Lett. (1998) 753.
- [11] G.P. Smestad, M. Grätzel, J. Chem. Educ. 75 (1998) 752.
- [12] K. Hara, M. Kurashige, S. Ito, A. Shinpo, S. Suga, K. Sayama, H. Arakawa, Chemical Communications, Cambridge, United Kingdom, 2003, p. 252.
- [13] K. Hara, M. Kurashige, Y. Dan-oh, C. Kasada, A. Shinpo, S. Suga, K. Sayama, H. Arakawa, New J. Chem. 27 (2003) 783.
- [14] P. Falaras, Sol. Energy Mater. Sol. Cells 53 (1998) 163.
- [15] N.W. Duffy, K.D. Dobson, K.C. Gordon, B.H. Robinson, A. McQuillan, J. Chem. Phys. Lett. 266 (1997) 451.
- [16] T. Ma, K. Inoue, K. Yao, H. Noma, T. Shuji, E. Abe, J. Yu, X. Wang, B. Zhang, J. Electroanal. Chem. 537 (2002) 31.
- [17] Y.-X. Weng, L. Li, Y. Liu, L. Wang, G.-Z. Yang, J. Phys. Chem. B 107 (2003) 4356.
- [18] P. Pechy, F.P. Rotzinger, M.K. Nazeeruddin, O. Kohle, S.M. Zakeeruddin, R. Humphry-Baker, M. Grätzel, J. Chem. Soc., Chem. Commun. (1995) 1093.
- [19] P. Pechy, F.P. Rotzinger, M.K. Nazeeruddin, O. Kohle, S.M. Zakeeruddin, R. Humphry-Baker, M. Grätzel, J. Chem. Soc., Chem. Commun. (1995) 65.
- [20] C.A. Bignozzi, R. Argazzi, C. Kleverlaan, J. Chem. Soc. Rev. 29 (2000) 87.
- [21] T. Ma, K. Inoue, H. Noma, K. Yao, E. Abe, J. Mater. Sci. Lett. 21 (2002) 1013.
- [22] K. Kalyanasundaram, N. Vlachopoulos, V. Krishnan, A. Monnier, M. Grätzel, J. Phys. Chem. 91 (1987) 2342.
- [23] R. Dabestani, A.J. Bard, A. Campion, M.A. Fox, T.E. Mallouk, S.E. Webber, J.M. White, J. Phys. Chem. 92 (1988) 1872.
- [24] G.K. Boschloo, A. Goossens, J. Phys. Chem. 100 (1996) 19489.
- [25] S. Cherian, C.C. Wamser, J. Phys. Chem. B 104 (2000) 3624.
- [26] C.C. Wamser, Personal communication, 2003.
- [27] Y. Tachibana, S.A. Haque, I.P. Mercer, J.R. Durrant, D.R. Klug, J. Phys. Chem. B 104 (2000) 1198.
- [28] T.M.R. Viseu, G. Hungerford, M.I.C. Ferreira, J. Phys. Chem. B 106 (2002) 1853.
- [29] F. Odobel, E. Blart, M. Lagree, M. Villieras, H. Boujtita, N. El Murr, S. Caramori, C.A. Bignozzi, J. Mater. Chem. 13 (2003) 502.
- [30] T. Ma, K. Inoue, H. Noma, K. Yao, E. Abe, J. Photochem. Photobiol. A 152 (2002) 207.
- [31] C.A. Bignozzi, J.R. Schoonover, F. Scandola, Prog. Inorg. Chem. 44 (1997) 1.
- [32] R.B.M. Koehorst, G.K. Boschloo, T.J. Savenije, A. Goossens, T.J. Schaafsma, J. Phys. Chem. B 104 (2000) 2371.
- [33] F. Fungo, L. Otero, E.N. Durantini, J.J. Silber, L.E. Sereno, J. Phys. Chem. B 104 (2000) 7644.
- [34] F. Fungo, L.A. Otero, L. Sereno, J.J. Silber, E.N. Durantini, J. Mater. Chem. 10 (2000) 645.
- [35] M.E. Milanesio, M. Gervaldo, L.A. Otero, L. Sereno, J.J. Silber, E.N. Durantini, J. Porphyrins Phthalocyanines 7 (2003) 42.
- [36] M.E. Milanesio, M. Gervaldo, L.A. Otero, L. Sereno, J.J. Silber, E.N. Durantini, J. Phys. Org. Chem. 15 (2002) 844.
- [37] R.S. Loewe, R.K. Lammi, J.R. Diers, C. Kirmaier, D.F. Bocian, D. Holten, J.S. Lindsey, J. Mater. Chem. 12 (2002) 1530.
- [38] K. Kalyanasundaram, J.A. Shelnutt, M. Grätzel, Inorg. Chem. 27 (1988) 2820.
- [39] A. Kay, M. Grätzel, J. Phys. Chem. 97 (1993) 6272.
- [40] A. Kay, R. Humphry-Baker, M. Grätzel, J. Phys. Chem. 98 (1994) 952.
- [41] A. Sen, V. Krishnan, Tetrahedron Lett. 37 (1996) 8437.
- [42] A.K. Burrell, D.L. Officer, D.C.W. Reid, Angew. Chem. Int. Ed. Engl. 34 (1995) 900.
- [43] A.K. Burrell, D.L. Officer, Synlett (1998) 1297.
- [44] E.E. Bonfantini, A.K. Burrell, W.M. Campbell, M.J. Crossley, J.J. Gosper, M.M. Harding, D.L. Officer, D.C.W. Reid, J. Porphyrins Phthalocyanines 6 (2002) 708.
- [45] A.K. Burrell, D.L. Officer, P.G. Plieger, D.C.W. Reid, Chem. Rev. 101 (2001) 2751.
- [46] Manuscript in preparation.
- [47] Philips Halotone Master Line Plus, GU 5.3, 12V/50W Halogen bulb, 24° Beam (UV Block).
- [48] K. Kalyanasundaram, Photochemistry of Polypyridine and Porphyrin Complexes, Academic Press Limited, England, 1992.
- [49] K.M. Smith (Ed.), Porphyrins and Metalloporphyrins, second ed., Elsevier, Amsterdam, 1975.
- [50] D.C.W. Reid, Ph.D. Thesis, IFS Chemistry, Massey University, Palmerston North, New Zealand, 1998.
- [51] M.K. Nazeeruddin, S.M. Zakeeruddin, R. Humphry-Baker, M. Jirousek, P. Liska, N. Vlachopoulos, V. Shklover, C.-H. Fischer, M. Grätzel, Inorg. Chem. 38 (1999) 6298.